

4-26-2016

Evaluation of Alternative Implementation Methods of Failure Sampling Approach for Structural Reliability Analysis

Kapil Patki

Wayne State University, kapil.patki@wayne.edu

Christopher D. Eamon

Wayne State University, eamon@eng.wayne.edu

Recommended Citation

Patki, K., & Eamon, C. (2016). Evaluation of Alternative Implementation Methods of a Failure Sampling Approach for Structural Reliability Analysis. *ASCE-ASME Journal of Risk and Uncertainty in Engineering Systems, Part A: Civil Engineering*, 2(4), 04016004. doi:10.1061/AJRUA6.0000876

Available at: https://digitalcommons.wayne.edu/ce_eng_frp/29

This Article is brought to you for free and open access by the Civil and Environmental Engineering at DigitalCommons@WayneState. It has been accepted for inclusion in Civil and Environmental Engineering Faculty Research Publications by an authorized administrator of DigitalCommons@WayneState.

Evaluation of Alternative Implementation Methods of Failure Sampling Approach for Structural Reliability Analysis

Kapil Patki¹ and Christopher Eamon²

Abstract

In this paper, several alternative approaches are used to implement the failure sampling method for structural reliability analysis and are evaluated for effectiveness. Although no theoretical limitation exists as to the types of problems that failure sampling can solve, the method is most competitive for problems that cannot be accurately solved with reliability index-based approaches and for which simulation is needed. These problems tend to have non-smooth limit state boundaries or are otherwise highly nonlinear. Results from numerical integration and three extrapolation approaches using the generalized lambda distribution, Johnson's distribution, and generalized extreme value distribution are compared. A variety of benchmark limit state functions were considered for evaluation where the number of random variables, degree of non-linearity, and level of variance were varied. In addition, special limit state functions as well as two complex engineering problems requiring nonlinear finite element analysis for limit state function evaluation were considered. It was found that best results can be obtained when failure sampling is implemented with an extrapolation technique using Johnson's distribution, rather than with numerical integration or the generalized lambda distribution as originally proposed with the method.

1. PhD Student, Dept. of Civil & Environmental Engineering, Wayne State University, Detroit, MI 48202; kapil.patki@wayne.edu.
2. Associate Professor of Civil and Environmental Engineering, Wayne State University, Detroit, MI 48202; eamon@eng.wayne.edu

Introduction

Reliability analysis of complex engineering problems, such as those requiring finite element analysis, often demand high computational costs. Both simulation-based methods, such as Monte Carlo Simulation (MCS) and its variants, as well as reliability index approaches such as the First Order Reliability Method (FORM), have been popular choices for structural reliability analysis. FORM and similar methods such as the Second Order Reliability Method (SORM) (Rackwitz and Fiessler 1978; Breitung 1984) rely on identifying the most probable point of failure (MPP) on the failure boundary. Reliability index β is commonly used in structural reliability analysis to quantify structural safety rather than failure probability directly. It is usually calculated as the distance between the MPP and the origin in standard normal space, where the MPP represents the location of the largest value of the joint probability density function that lies upon the failure boundary of the limit state function. Although computationally efficient, these methods may provide poor solutions for problems nonlinear in standard normal space caused by the linearization of the limit state function at the MPP (Eamon et al. 2005; Melchers 1999; Chiralaksanakul and Mahadevan 2005; Haldar and Mahadevan 2000). Moreover, search algorithms sometimes cannot identify the MPP for complex problems that may be highly non-linear, discontinuous, or that have multiple ‘local’ MPPs on the failure boundary (Eamon and Charumas 2011). In such cases, if the MPP cannot be found, the reliability index-based methods will fail to provide any solution.

To reduce the cost of simulation methods but maintain reasonable accuracy, numerous variance reduction techniques were developed such as stratified sampling (Iman and Conover 1982), importance sampling (Rubinstein 1981; Engelund and Rackwitz 1993) and adaptive importance sampling (Wu 1992; Karamchandani et al. 1989). However, stratified sampling techniques such as Latin Hypercube (Iman and Conover 1982) have not consistently shown

significant reductions in computational costs; and as importance sampling methods also rely on identifying the MPP, they may also fail to provide solutions, or provide poor solutions, for complex limit states. Various other simulation methods that do not rely upon the MPP have been proposed, such as subset simulation (Au and Beck 2001; Au et al. 2007) and directional simulation (Ditlevesen and Bjerager 1988), among many others. Although directional simulation can perform extremely well in some cases, such as when the limit state boundary approaches a spherical shape, it is not particularly efficient when the boundary takes a planar form or small multiples thereof (Engelund and Rackwitz 1993). A significant body of research has been conducted on the development of subset simulation methods, and multiple competing versions exist. An important consideration with this method, however, is proper selection of the importance sampling density, some choices of which can be associated with high variance in the solution (Au and Beck 2001; Au et al. 2007).

Alternatively, rather than refine the reliability method, a response surface technique can be used to represent a computationally expensive limit state function with a simpler, analytical surrogate function (Gomes and Awruch 2004; Cheng and Li 2009). Once formed, the response surface can be used to provide very fast reliability solutions. However, these techniques often require high computational effort to develop accurate responses for highly non-linear or discontinuous limit state functions, a cost which may outweigh the savings gained with their use (Eamon and Charumas 2011).

As an alternative solution for complex reliability problems, this paper examines the use of a modified conditional expectation approach proposed by Eamon and Charumas (2011), 'failure sampling.' The method was reportedly used to accurately solve various complex limit states with reasonable computational effort. The approach offers several useful features: (1) as there is no reliance on the MPP, complex problems for which the MPP cannot be accurately located, and thus are unsolvable or poorly solved by methods such as

FORM, SORM and importance sampling, can be addressed; (2) for many complex, moderate reliability (i.e. reliability index from 3-5) problems that are poorly solved with many other methods, computational effort for failure sampling is relatively low; (3) efficiency does not vary significantly among different types of problems of the same reliability level; and (4) the method is mathematically simple and straightforward to implement.

It should be emphasized that, as a simulation-based method, although it can be theoretically applied to problems of any complexity or reliability level, failure sampling is most effective for problems that are complex and for which reliability index-based methods provide no or poor solutions, and for which other simulation methods require an unfeasibly large computational effort. For practical implementation, two observations can be noted. First, earlier work, as well as the results of this study, have found that no more than 1000 simulations are usually sufficient to solve a wide range of complex problems with reliability indices from 3-5 and sometimes higher (Eamon and Charumas 2011). Increasing the number of simulations will correspondingly increase the precision of the solution as well as the reliability level that can be addressed. Second, for problems that can be solved accurately with non-simulation methods such as FORM (typically, problems that are simple; i.e. smooth limit state boundaries that are not highly nonlinear in standard normal space), failure sampling is usually not competitive, as reliability index-based approaches can typically accurately solve simple problems with many fewer calls to the limit state function than can a simulation approach. Thus, for simpler problem types and for problems with low reliability, other methods are generally more efficient.

The failure sampling solution process can be implemented in various ways. In previous work, the numerical integration and generalized lambda distribution fit methods were used, which are described in the next section. In this study, several alternative methods

are considered, and results superior to those originally presented by Eamon and Charumas (2011) are identified.

Summary of Failure Sampling

The starting point for a conditional expectation solution is to construct a data sample of random variables (X_j) that only lies upon the failure boundary of a limit state function $g(X_j)$. This is achieved by simulating values of all random variables except one (Q) (call this remaining, realized set of random variables (x_i)), then determining the value q that sets $g = 0$. As the resulting complete set of (x_j) (containing (x_i) and q) is biased due to the non-random values determined for Q , (x_j) is not used to directly compute failure probability p_f as with the traditional MCS process (as this would always result in $p_f = 1.0$). In the failure sampling process, values for Q are not of interest; Q is a single random variable with statistical properties that are expected to be fully defined. Rather, assuming the problem has multiple random variables and is somewhat complex, a statistical description of the random function within g containing the variables other than Q , $R(X_i)$, is of interest, which can be found by obtaining values for Q , as described using the process below. The advantage of sampling $R(X_i)$ only rather than sampling g directly with all RVs (X_j), such as in the traditional MCS process, is significant. In particular, only sampling $R(X_i)$ allows the failure region of the problem to be more easily captured, as shown in Figure 1. The complete approach is fully described elsewhere (Eamon and Charumas 2011), whereas a step-wise summary of the procedure is provided here.

1. From an original limit state function $g(X_j)$ with random variables (X_j), a control random variable Q is chosen. A new limit state function g^* is then formed such that it has an equivalent failure boundary to that of $g(X_j)$, but Q is separated from the remaining random variables. That is, at failure, $g(X_j)$ is expressed as:

$$g^* = R(X_i) - Q = 0 \quad (1)$$

Here, $R(X_i)$ is the portion of the limit state function that is not a function of Q , and (X_i) is the set of all random variables (X_j) except Q . There is no theoretical limitation to the selection of Q , although it is best that Q is selected such that it is statistically independent of the remaining random variables (X_i) . For example, consider a simple limit state function $g = X_1X_2 - X_3/X_4$. Assume X_3 is chosen as the control variable Q . A new limit state boundary is then written as $g^* = 0 = X_1X_2X_4 - X_3$. Here, $X_1X_2X_4 = R(X_i)$ and $X_3 = Q$. In a more realistic, complex case, g^* can only be expressed implicitly, such as: $g^* = f(X_i, Q)$, where the evaluation of $f(X_i, Q)$ requires a numerical method such as finite element analysis. This implicit form causes no theoretical difficulty, as g^* need not be explicitly expressed in terms of (X_i) and Q . However, implicit forms of g^* will require the use of a nonlinear solver to set $g^* = 0$, as discussed in step 3 below.

2. Random values for variables within R , (X_i) (i.e. all random variables except Q) are simulated. In this paper, direct MCS is used for the simulation. $R(X_i)$ is then evaluated. For the example above, MCS would be used to simulate values x_1 , x_2 , and x_4 for random variables X_1 , X_2 , and X_4 , respectively.

3. Based on the set of realized random variable values (x_i) in step 2, the value of Q needed to satisfy Eq. 1, (q) , is determined. For simple problems that can be written explicitly as $g^* = 0 = R(X_i) - Q$, this is simply $q = R(x_i)$. For implicit, nonlinear problems, such as $g^* = f(R(X_i), Q)$, to find a value q such that $g^* = f(R(x_i), q) = 0$, no closed-form solution exists, and some type of nonlinear solver must be used. In general, q is incrementally increased (or decreased) until the limit state g^* equals zero. For this study, the bisection method is used with 1%-3%

tolerance to satisfy Eq. 1 for such problems, as discussed in more detail in example problem 3, below.

4. Steps 2-3 are repeated until a sufficient number of values for Q have been determined. In this paper, 1000 simulations were used. At this point, there is no need to evaluate the true response further. Notice that, since $q = R(x_i)$ per step 3, the values of q that were determined also equal values of $R(x_i)$ on the failure boundary. That is, a data sample representing the random function $R(X_i)$ with variables (X_i) (i.e. all but Q) has been established.

5. The data sample for $R(x_j)$ is further manipulated in one of two ways. In the first process, the numerical integration approach, a probability density function (PDF) estimate of the data is developed. This PDF is then numerically integrated to form a cumulative distribution function (CDF). As discussed in Eamon and Charumas (2011), rather than forming a CDF directly from the $R(x_i)$ data sample, developing a PDF first tends to reduce variance in the solution. As recommended, when considering the integration approach, the PDF estimate was formed from 50 intervals, creating a 50-point CDF upon integration. The second method in which the $R(x_i)$ data can be manipulated is by replacing the data completely with an analytical curve. If the curve is highly flexible and can fit the data well, this approach has the advantage of extending the tail of $R(x_i)$ beyond that which was originally generated.

6. Failure probability is estimated. Two general approaches exist, depending on the method used to manipulate the $R(x_i)$ data in step 5. Notice that, with the statistical parameters of $R(X_i)$ estimated, the limit state function is effectively reduced to a two random variable problem given by: $g^* = R - Q$, where the potentially complex (and possibly implicit) $R(X_i)$ is now represented explicitly as a single random variable R .

Considering the first method for solution, if the numerical integration approach discussed in step 5 was used to form a CDF of $R(x_i)$, the most straightforward way to compute p_f is to simply numerically integrate the well-known expression:

$$p_f = \int_{-\infty}^{\infty} F_R(x) f_Q(x) dx \quad (2)$$

In Eq. 2, $F_R(x)$ refers to the estimated CDF of $R(x_i)$, found per step 5, and $f_Q(x)$ is the PDF of Q .

Alternatively, if the original $R(x_i)$ data are represented with an analytical distribution, p_f (or reliability index β) of $g^* = R - Q$ can be quickly calculated with one of many available simple reliability methods, such as MCS or FORM, as the original, potentially complex multi-variate function g is now represented analytically as an equivalent, simple and analytical two random variable problem with R and Q fully defined. With this approach, for this study, MCS was used to compute p_f of g^* , then results reported in terms of reliability index β with the transformation $\beta = -\Phi^{-1}(p_f)$, where Φ is the standard normal CDF. Notice that β essentially represents the number of standard deviations from the mean of a standard normal random variable associated with the given failure probability. Although transformation from p_f to β is not necessary, reliability index is the standard metric of safety in structural reliability analysis rather than p_f directly, which is often numerically cumbersome. Note that typical notional reliability indices of components designed by prevailing structural engineering Load and Resistance Factor Design standards are generally between 2 and 4 (Rosowsky et al. 1994; Eamon and Nowak 2005; Szerszen and Nowak 2003)).

Implementation Methods Considered

In this study, after forming the $R(x_i)$ data sample, several alternative analytical distributions were used to represent $R(x_i)$: the generalized lambda distribution (GLD),

Johnson's distribution (JSD), and the generalized extreme value distribution (GEV).

The generalized lambda distribution is a four parameter distribution known for its high flexibility, and can represent many common distributions such as normal, lognormal, Weibull, etc. (Karian and Dudewicz 2011). The distribution is defined by four parameters: λ_1 , λ_2 , λ_3 , and λ_4 . Parameters λ_1 and λ_2 are location and scale parameters, respectively, while λ_3 and λ_4 describe skewness and kurtosis. The distribution can be defined as follows. Given the quantile function $Q(u) = \lambda_1 + \frac{u^{\lambda_3} - (1-u)^{\lambda_4}}{\lambda_2}$ (the inverse of the CDF), at $x = Q(u)$, where input parameter u refers to probability (i.e. from 0 to 1), the PDF of the generalized lambda distribution is given by:

$$f_R(x) = \frac{\lambda_2}{[\lambda_3 u^{(\lambda_3-1)} + \lambda_4 (1-u)^{(\lambda_4-1)}]} \quad (3)$$

There are numerous methods to determine the parameters of the distribution (Karian and Dudewicz 2011; Ozaturk and Dale 1985; Asif and Helmut 2000). For this study, the method of moments was used (Karian and Dudewicz 2011). This process makes use of expressions that relate parameters $\lambda_1 - \lambda_4$ to the first four sample moments. However, these expressions are implicit, and due to the algebraic complexity of the relationships, direct solution of $\lambda_1 - \lambda_4$ is generally not possible, and numerical methods are commonly employed. In a typical numerical process, values for λ_3 and λ_4 are first found by minimizing the difference between the generalized lambda distribution moments and the sample moments, while constraining results to a feasible solution space. In this study, a sequential quadratic programming optimization technique is used to solve the minimization problem. Once λ_3 and λ_4 are determined, the relationships among $\lambda_1 - \lambda_4$ and the sample moments described above can be sufficiently simplified such that the remaining parameters λ_1 and λ_2 can be found algebraically (Karian and Dudewicz 2011).

In some cases, changing the method used to determine the generalized lambda distribution curve parameters may influence the resulting quality of fit. In addition to the method of moments, other common methods of determining curve parameters for the generalized lambda distribution include the method of percentiles and the method of L-moments. Some have found that the method of percentiles gives superior results to the method of moments when sample moments are computed with higher levels of uncertainty; i.e. usually when considering small sample sets and large coefficients of variation (Karian and Dudewicz 2011). However, the authors of this study found no significant advantage with the method of percentiles over the method of moments for fitting the generalized lambda distribution to the problems considered. Although the method of L-moments has been shown to provide good results in some cases, it was generally found to produce inferior results for the generalized lambda distribution when compared to the method of percentiles (Karian and Dudewicz 2003), and was thus not considered further in this study.

Similar to the generalized lambda distribution, the Johnson system of distributions is defined by four parameters and has significant flexibility to cover a wide variety of shapes. The Johnson system is based on three possible transformations of a normal random variable in addition to the identity transformation. The ‘SB’ transformation represents a bounded distribution, the ‘SL’ transformation represents a semi-bounded distribution, and the ‘SU’ transformation represents an unbounded distribution in the Johnson system. Transformation from a standard normal random variable Z to a Johnson random variable X for the SB, SL and SU transformations can be represented as follows:

$$X = \xi + \lambda_j \cdot \Gamma^{-1} \left(\frac{Z - \gamma}{\delta} \right) \quad (4)$$

where Γ denotes the transformation function, γ and δ are the shape parameters, ξ is the location parameter, and λ_j is the scale parameter. The resulting PDF is given by:

$$f_R(x) = \frac{\delta}{\lambda_j \sqrt{2\pi}} g' \left(\frac{x - \xi}{\lambda_j} \right) \exp \left[-\frac{1}{2} \left(\gamma + \delta g \left(\frac{x - \xi}{\lambda_j} \right) \right)^2 \right] \quad (5)$$

where $g(y) = \ln(y)$, $\ln(y/(1-y))$, and $\ln(y+(y^2+1)^{1/2})$ for the SL, SB, and SU transformations, respectively, and $Y = (X - \xi) / \lambda_j$. The ‘SN’ transformation is the identity transformation and represents a normal distribution. Although various methods to determine the parameters of the Johnson distribution are available, the method of moments, method of percentiles, and method of quantile estimators are common. In this research, the method of percentile estimators was used (Karian and Dudewicz 2011; George 2007; Slifker and Shapiro 1980), as it was found that the method of moments produced less accurate estimations of the third and fourth moment parameters for the Johnson distribution, particularly when the sample size becomes small. In the percentile method, specified percentiles of the standard normal distribution are matched with corresponding percentile estimates of the sample. More specifically, using the process described by Slifker and Shapiro (1980), the parameters of the distribution are determined by solving the transformation function Γ at four different percentiles, where the percentiles of the standard normal variate are taken between three intervals of equal length at points $\pm z$ and $\pm 3z$. Based on the calculated discriminant value between the percentiles, a best-fit Johnson family can be selected, and with explicit expressions available in the literature (Slifker and Shapiro 1980), the corresponding distribution parameters are readily determined.

The generalized extreme value distribution combines three simpler distributions into a single form, allowing a continuous range of possible shapes weighted among the component distributions. Similar to the extreme value distribution, the generalized type is often used to model the smallest or largest values in a large set of independent data. It is defined by a location parameter μ , a scale parameter σ , and a shape parameter k , where k takes on a value other than zero. The PDF of the distribution is described by:

$$f_R(x) = \frac{1}{\sigma} \exp\left(-\left(1 + k \frac{(x - \mu)}{\sigma}\right)^{\frac{-1}{k}}\right) \left(\left(1 + k \frac{(x - \mu)}{\sigma}\right)^{-1 - \frac{1}{k}}\right) \quad (6)$$

The parameters of the distribution were determined using similar techniques as those used for the Johnson distribution.

Comparison Problems and Results

As noted in the introduction, the purpose of this study is to investigate the effectiveness of different methods of implementing failure sampling, and perhaps to lead to additional improvements in method accuracy and/or efficiency. As such, it is desirable to investigate the performance of the implementation methods with a variety of different reliability problems. For such an evaluation to be feasible, the true solution of the problems must be readily verifiable. Therefore, some of the problems investigated are benchmark reliability problems taken from the literature. As established benchmark problems, these can be effectively solved with existing reliability approaches, and a failure sampling solution is not needed, nor does it represent the most efficient solution for some of these problems. Nevertheless, the solution of such problems can provide valuable information as to the effectiveness of the investigated implementation approaches for different problem types. However, as failure sampling was specifically intended for complex, more realistic engineering problems, two problems of this type were also considered, both of which involve nonlinear finite element analysis for the evaluation of the limit state function (problems 3 and 4). In order to identify potential differences in the implementation methods, a relatively small number of simulations (1000) was used to solve all problems, even those with a reliability index approaching 4 (p_f approximately 1:30,000). Although very reasonable solutions can be obtained with this small number of simulations for even higher reliability

indices, if desired, additional accuracy and precision can be achieved by increasing the number of simulations.

Problem Series 1: Flexible Limit State Function

This function is taken from Eamon et al. (2005) and is used to evaluate the effect of varying the number of random variables (RVs), distribution type, level of variance, problem linearity, and target reliability level. Specific parametric variations included: 2, 5, and 15 RVs; coefficients of variation of 5% and 35%; normal, lognormal, and extreme type I distributions; algebraic linearity, where linear, moderately nonlinear, and highly nonlinear limit states were considered; and target reliability index, where ‘low’ and ‘high’ values were considered, ranging from 0.3 - 5.0. Various combinations of these different parameters resulted in a total of 72 different limit state functions for consideration. The general form of the limit state function is given as:

$$g = k \sum_{i=1}^n d_i - c \sum_{j=1}^k \frac{L_j^A w_j}{E_j I_j} \quad (7)$$

Parameters taken as RVs are given in Table 1, while values for the parameters are given in Table 2, and have been used either as the mean value if an RV, or a constant value if a non-RV, depending on the case type. All cases were evaluated with failure sampling using numerical integration (abbreviated as “NI” in the figures and tables), and the generalized lambda, Johnson, and generalized extreme value distribution implementations. Results are measured in terms of accuracy and precision, where accuracy is the mean value of the ratio of computed reliability index to the exact value for the specific case under consideration. The exact value for low to moderate target reliability indices is determined from 1×10^6 MCS simulations, and for high target reliability index cases, the exact value is determined from 1×10^9 MCS simulations. Precision is used to measure the degree of consistency of results, and is

determined by calculating the coefficient of variation (COV) of accuracy, based on five evaluations of each problem. Figures 2-7 show the effect of number of RVs, degree of non-linearity, and RV distribution type on the different implementation methods.

Figures 2 and 3 concern the effect of linearity. As shown, it was found that varying linearity had little effect on solution quality. Considering differences among methods, by a slight margin, the generalized lambda distribution produced the best overall results for accuracy (Figure 2), generating error within 1% for all cases (where throughout this study, % error is taken as the absolute value of: $(\text{exact value} - \text{calculated}) \times 100 / \text{exact value}$). However, the Johnson distribution produced nearly the same results with the exception of one case (nonlinear, low reliability), at 4% error. Numerical integration and the generalized extreme value distribution provided less consistent accuracy from case to case, and the generalized extreme value distribution performed worse overall, with three cases from 5-8% error. For precision (Figure 3), the Johnson distribution generated best results overall, with only 5-6% COV in the solution when using 1000 simulations. The generalized lambda distribution was somewhat worse, with COV from 8-10%. Similar to the results for accuracy, numerical integration and the generalized extreme value distribution were most variable from case to case for precision, with the generalized extreme value distribution results again worse overall, with about 10-12% COV.

Generally, as shown in Figures 4 and 5, increasing the number of RVs also had no significant effect on solution outcome. However, the 15 RV, high reliability case was generally least precise for all methods. The generalized lambda and Johnson distributions produced nearly the same accuracy (Figure 4), with about 4% error or less for all cases. One exception is the 15 RV high reliability case, for which the Johnson distribution generated 7% error. Similar to previous results, numerical integration and the generalized extreme value distribution were found to have the most variation and highest error in results, where in two

cases (5 RV, low reliability for the generalized extreme value distribution and 15 RV, high reliability for numerical integration), error approached a very high 20%. Regarding precision (Figure 5), the Johnson distribution was shown to produce best results overall, where COV ranged from 3-6% in all cases except one (15 RV, high reliability) and COV was approximately 10%. However, all other methods produced higher solution variance with this case as well, with COV from about 12-14%. The generalized lambda distribution performed worse overall for precision, ranging from about 12-15% COV. As with previous results, significant variation was found among cases with both numerical integration and the generalized extreme value distribution, ranging from 2-14% COV depending on problem type.

As with previous results, altering RV distribution normality, as shown in Figures 6 and 7, did not degrade the solution. As shown in Figure 6, only minor variations in accuracy were found among different methods. One exception is the normal, high reliability case, for which the Johnson distribution produced a relatively high error at about 9%. For precision (Figure 7), results were again similar for most methods, producing about 4-6% COV. Overall, the generalized lambda distribution appears best, with most cases at 4% COV. However, results from the Johnson distribution are more consistent among cases, though with a slightly higher typical COV at about 6%. As with some previous results, most variation from case to case occurred with numerical integration and the generalized extreme value distribution.

In summary, the results show that most implementation methods produced reasonably accurate results for most cases, though precision suffered in some cases when limiting the sample to 1000 simulations. In particular, the generalized extreme value distribution demonstrated relatively poor precision for nonlinear limit states and for high reliability cases, while the generalized lambda distribution implementation lacked precision in general relative

to the other approaches. As expected, all methods were accompanied by a decrease in precision for high reliability cases with a high number of RVs. Though a few exceptions exist, overall, the most accurate and consistent results were found with the Johnson distribution. Surprisingly, the cases where the Johnson distribution yielded lowest accuracy were linear limit state functions. However, these cases were those with 15 RVs and high beta values. It was also found that the precision of numerical integration, the generalized lambda distribution and the generalized extreme value distribution decreased most when the number of RVs increased. Here, the generalized lambda and generalized extreme value distributions failed to provide a good fit for highly non-linear cases with 15 RVs. For the generalized lambda distribution, this can be attributed to a poor representation of skewness and kurtosis of the distribution for the limited size of the $R(x_i)$ sample taken. The generalized extreme value distribution, however, poorly represented the tail region.

Problem Series 2: Special Limit State Functions

Engelund and Rackwitz (1993) presented a series of unique, often difficult to solve limit state functions. The results of two of these functions found to be most challenging for the methods considered in this paper are presented below.

Multiple Reliability Indices:

This hyperbolic limit state function has two reliability indices, and is given as:

$$g = x_1 x_2 - 146.14 \quad (8)$$

where x_1 and x_2 are normal RVs having mean values of 78064.4 and 0.0104, with corresponding standard deviations of 11709.7 and 0.00156, respectively. Results are presented in Table 3, where it can be observed that only numerical integration and the Johnson distribution could produce results, whereas the generalized lambda and generalized extreme value distributions failed to fit the $R(x_i)$ sample. As shown, both accuracy and

precision for numerical integration and the Johnson distribution are similar, with numerical integration slightly superior (exact solution obtained from 1×10^9 MCS samples). For comparison, MCS and FORM solutions (limited to the same computational effort as the failure sampling approaches) are given as well; neither could produce a viable solution for this problem.

Maximum Function:

This limit state function is expressed as the maximum of several sub-functions, and is given by the following expression:

$$g = \max(g_1, g_2, g_3, g_4) \quad (9)$$

where:

$$g_1 = 2.677 - u_1 - u_2$$

$$g_2 = 2.500 - u_2 - u_3$$

$$g_3 = 2.323 - u_3 - u_4$$

$$g_4 = 2.250 - u_4 - u_5$$

All u_i are standard normal random variables. As with the previous example, as shown in Table 4, the generalized lambda and generalized extreme value distributions were unable to fit the data, whereas numerical integration and the Johnson distribution produced reasonable results. In this case, the Johnson distribution produced the greatest accuracy and precision (exact solution obtained from 1×10^9 MCS samples).

Problem 3: Non-Linear Truss

This problem is based on that described in Eamon and Charumas (2011), and is meant to represent complexity in the range of that for which the failure sampling approach is intended. As shown in Figure 8, a 10 member non-linear truss is subjected to a load P . Solution of the problem cannot be achieved with a closed-form analytical expression, and a

finite element code (ABAQUS) was used to evaluate the response. Two different limit states were considered for this problem: one in terms of displacement, and another in terms of stress. The material was taken as steel, with a bilinear stress-strain curve and an elastic modulus E of 200 GPa (29,000 ksi). For the displacement-based limit state problem, only three RVs were considered: yield stress (σ_y), post-yield modulus (E_2), and load (P). RVs σ_y and E_2 are considered to be the same for all truss members, with means of 345 MPa (50 ksi) and 8.28 GPa (1200 ksi), and COVs of 0.10 and 0.25, respectively. To vary reliability index, two values of P were considered: 223 and 267 kN (50 and 60 kips), with COV of 0.10. A third variation of this problem was considered as well in which resistance RVs (σ_y , E_2 , P) were taken as partially correlated ($\rho=0.50$), and COV of each increased to 0.35. In all problems, failure is defined as the state where displacement at the point of load application exceeds 1.5 inches. Hence, the limit state function is given as:

$$g = 1.5 - D(\sigma_y, E_2, P) \quad (10)$$

All RVs are taken as normally distributed, and P was considered to be the control variable. The bisection method was used to solve for the condition $g^* = 0$ (Eq. 1), with an error tolerance of 1% in one case and 3% in a second case, for comparison. The method works by bracketing the solution, then refining the solution estimate with subsequent linear interpolations that narrow the bracket. Note that although the limit state function was evaluated with a sample size of 1000 (the "nominal" number of calls given in the results tables), the actual number of function calls (the "actual" number of calls given in the tables) exceeded this value, due to the iterative process needed to find the root of $g^* = 0$. More sophisticated root finding techniques are available that can decrease the actual number of calls further, improving solution efficiency. However, this is a topic beyond the scope of this paper. For fair comparison, the actual number of calls is kept constant for all methods, such that total computational effort is the same.

A more complex version of the problem was also considered, where the limit state function was reformulated in terms of stress. In this case, each member of the truss was associated with three independent RVs, resulting in a total of 31 RVs for the problem. RVs are cross-sectional area A (mean = 1290 mm² (2 in²), COV = 0.05), and the previous RVs of yield stress σ_y and post yield modulus E_2 , with the same statistical parameters used in the displacement problem. The mean value of load P (the control variable) was taken as 223 kN (50 kips) in one version of the problem and 289 kN (65 kips) in another, to vary target reliability index, with COV of 0.1. A third variation was also considered in which resistance RVs were taken as partially correlated (coefficient of correlation $\rho= 0.30$) for area RVs, yield stress RVs ($\rho= 0.50$), and for post-yield modulus RVs ($\rho= 0.70$), while the COV of the post-yield modulus RVs was increased to 0.30. The failure criterion was defined as the state where the stress in member 1 reaches its yield stress. The resulting limit state function is given as:

$$g = \sigma_{y1} - \sigma_1(P, \sigma_{yj}, E_{2i}, A_i) \text{ for } i = 1 \text{ to } 10, j = 2 \text{ to } 10 \quad (11)$$

The exact solution was obtained from 1×10^9 MCS samples, which required approximately 400 CPU hours. Tables 5 and 6 show the results obtained for the displacement and stress limit state functions, respectively. For comparison, and to verify the suitability of problem complexity, a FORM solution was also attempted. This resulted in relatively high errors or solution failure for the displacement problems (Table 5) and failed to provide solutions for the stress problems (Table 6), as the MPP could not be located. Similarly, no solution could be obtained from MCS for the higher reliability cases when limiting the actual number of function calls to that used by the failure sampling implementation methods.

For the displacement limit case (Table 5), all failure sampling implementation methods produced reasonable results (1-5% error) for the low reliability level case ($P = 267$ kN) except numerical integration, where error was approximately 9%. For the higher

reliability case ($P = 223$ kN), only numerical integration and the Johnson distribution could solve the problem, with similar, relatively low error from 2-3% for the high (3%) $g^* = 0$ tolerance, and about 0.5% error for the low $g^* = 0$ (1%) tolerance alternative. Of course, the higher accuracy associated with lower $g^* = 0$ error tolerance is accompanied by higher simulation cost, which increased from 5000 to 8000 actual simulations, as shown. For the correlated, high COV RV case, the performance of numerical integration markedly decreased, producing a large error of approximately 25%. However, the Johnson distribution solution was not significantly affected, producing less than 3% error.

Considering the stress limit case (Table 6), as with the previous displacement limit problem, all methods generated reasonable solutions for the low reliability case except for numerical integration, where error exceeded 7% for the high $g^* = 0$ error tolerance case. However, for the higher reliability case ($P = 200$ kN), only the Johnson distribution could produce a solution for both high and low $g^* = 0$ error tolerance levels. In both cases, error was relatively low, from about 1-3%. Only the Johnson distribution and numerical integration could provide solutions for the correlated, high COV RV case. Here, the Johnson distribution error was approximately 3%, while results for numerical integration significantly worsened to nearly 13% error.

In summary, only the implementation method using the Johnson distribution could provide consistent and reasonable solutions for each of the multiple versions of the problem that were considered.

Problem 4: Steel Frame

This problem considers a small structure representing a bay of a larger building, with dimensions 7.3 m by 7.3 m (24 ft by 24 ft) in plan and 14.5 m (48 ft) high. It is a four-story steel frame, with concrete floor slabs and four interior shear walls, as shown in Figure 9. Note that it is idealized for the purpose of numerical investigation and not meant to model an

actual structure. Beams and columns of the structure are modeled with frame elements and assigned W14X22 wide flange steel beam section properties. The floor slabs and shear walls were modeled as shell elements, with slab thickness of 300 mm (12 in). A bilinear stress-strain model for steel was used, with RVs taken as modulus of elasticity of steel, E_s , with mean of 200 GPa (29000 ksi) and COV of 0.1, and post-yield modulus of elasticity of steel, E_t , with mean of 8.3 GPa (1200 ksi) and COV of 0.1. Additional RVs are modulus of elasticity of concrete, E_c , with mean of 24 GPa (3500 ksi) and COV of 0.1, and a uniform pressure load P applied to the floor slabs, which was taken as the control variable, with mean of 3.35 or 4.31 kN/m² (70 or 90 psf), depending on target reliability index considered, with COV of 0.1. The failure criterion is defined as the state where displacement at any point on the fourth floor slab exceeds 50 mm (2 in). The limit state function is given as:

$$g = 2 - D(E_s, E_t, E_c, P) \quad (12)$$

All RVs were taken as normally distributed. The limit state function was evaluated using a commercial finite element analysis code (ABAQUS). Approximately 600 CPU hours were required for 1×10^9 MCS samples to evaluate the exact solution. Two variants of this problem with higher complexity were also considered. In the first variant, resistance RVs were taken as partially correlated ($\rho = 0.65$) and COV of all resistance RVs was increased to 0.35. For the second variant, the number of resistance RVs was significantly increased to 52. In this problem, each of the 4 building floor slabs was divided into 4 sections as shown in Figure 9, and assigned a different modulus RV, as well as each of the 4 core shear walls for each floor, for 32 RVs E_{ci} . The COV for each of these RVs was taken as 0.30, with $\rho = 0.30$. Additional RVs are 8 steel column elastic modulus RVs E_{si} and post-yield modulus RVs E_{ti} (16 RVs total), where COV was taken as 0.3 and $\rho = 0.50$, as well as a floor thickness RV t_i for each floor (4 total), with COV of 0.1 and $\rho = 0.70$.

Results for the more simple, 4 RV problems with uncorrelated RVs are shown in Table 7. As shown, it was found that all methods considered could provide reasonable solutions for the lower reliability case ($P = 400$ kN). However, for the higher reliability case ($P = 312$ kN), only the generalized lambda and Johnson distributions could provide solutions, with the Johnson distribution providing the lowest error at less than 4%. Considering the more complex problems in Table 8, it can be seen that in both cases (4 and 53 RV versions), only the Johnson distribution could produce a solution. Here, the more complex problems did not reduce the solution fidelity for the Johnson distribution, where error remains at 3-4%.

Conclusion and Recommendations

By coupling simple tools such as MCS, conditional expectation, and numerical integration and/or tail extrapolation, it was found that a wide variety of complex reliability problems can be consistently and accurately solved with reasonable computational effort using the modified conditional expectation approach implemented as failure sampling. Although no theoretical limitation exists to the types of problems that failure sampling can solve, the method has shown to be most useful for complex, computationally demanding reliability problems for which traditional methods may provide unacceptably inaccurate or unfeasibly computationally costly solutions, such as problems which have non-smooth limit state boundaries or that are otherwise highly nonlinear. In this study, an evaluation of alternative implementation methods was conducted. In particular, different approaches for estimating the PDF of the data sample, and the effect on the efficiency and accuracy of the solution were studied. In total, 85 limit state variations were investigated that covered a wide variety of problems, with parametric changes including the number of RVs, degree of non-linearity, and level of variance. In addition, several special limit state functions and two complex engineering problems requiring finite element analysis for limit state function

evaluation were considered. From the investigation, it was found that increased accuracy can be obtained, for a wider variety of problems, with the Johnson distribution implementation rather than the generalized extreme value distribution or from the direct numerical integration or generalized lambda distribution approaches as originally suggested by Eamon and Charmus (2011). In particular, unlike the three other methods considered, the Johnson distribution provided highly-accurate to reasonably-accurate solutions for every one of the problems evaluated in this study, even when greatly restricting computational effort.

In a small number of cases, other approaches provided superior results. These were a nonlinear, low reliability case and a case with a high number of normal RVs with high reliability, for which the generalized lambda distribution preformed best, as shown in example problem 1. In these cases, however, the advantage over the Johnson approach was relatively small. Therefore, if the failure sampling approach is considered for reliability analysis, the Johnson distribution implementation is generally recommended for use. If a potentially more refined selection procedure is desired, an appropriate goodness-of-fit test might be considered to estimate the expected effectiveness of a given approach for a particular problem. An error metric such as that proposed by Eamon and Charumas (2011), which is based on differences between actual data and candidate curve CDF values, might serve this purpose, though its use requires additional effort. Given the wide applicability of the Johnson implementation, however, and the few cases for which alternative approaches were found to have a slight advantage, use of such a refinement does not appear to be particularly beneficial.

Acknowledgements

Funding was provided for this study by the National Science Foundation under Research Award No. 1127698, support for which is gratefully acknowledged.

Nomenclature

| | |
|------------------|--|
| f_Q | PDF of Q |
| F_R | CDF of $R(X_j)$ |
| f_R | PDF of $R(X_j)$ |
| $g(X_j)$ | initial limit state function |
| g^* | failure sampling limit state function |
| p_f | failure probability |
| Q | control random variable |
| $Q(u)$ | GLD quantile function |
| $R(X_i)$ | random function within g^* excluding Q |
| R | $R(X_i)$ represented as a single equivalent RV |
| u | GLD PDF input parameter (probability) |
| β | reliability index |
| λ_i | GLD parameter |
| Φ | standard normal CDF |
| Γ | transformation function for JSD |
| γ, δ | shape parameter for JSD |
| ξ | location parameter for JSD |
| λ_j | scale parameter for JSD |
| k | shape parameter for GEV |
| μ | location parameter for GEV |
| σ | scale parameter for GEV |

References

- Asif L, and Helmut M. (2000). "Estimating The Parameters Of The Generalized Lambda Distribution." *ALGO Research Quarterly*, Vol. 3, p. 47-58.
- Au SK, and Beck JL. (2001). "Estimation Of Small Failure Probabilities In High Dimensions By Subset Simulation." *Probabilistic Engineering Mechanics*, Vol. 16, p. 263-277.
- Au SK, Ching J, and Beck JL. (2007). "Application Of Subset Simulation Methods To Reliability Benchmark Problems." *Structural Safety*, Vol. 29, p. 183-193.
- Ayyub BM, and Chia CY. (1992). "Generalized Conditional Expectation For Structural Reliability Assessment." *Structural Safety*, Vol. 11, p. 131-146.
- Ayyub BM, and Haldar A. (1984). "Practical Structural Reliability Techniques." *ASCE Journal of Structural Engineering*, Vol. 110, p. 1707-1724.
- Breitung K. (1984) "Asymptotic Approximations for Multinormal Integrals." *ASCE Journal of Engineering Mechanics*, Vol. 110, p. 357-366.
- Cheng J, and Li QS. (2009). "Application Of Response Surface Methods To Solve Inverse Reliability Problems With Implicit Response Functions." *Computational Mechanics*, Vol. 43. p. 451-459.
- Chiralaksanakul A, and Mahadevan S. (2005). "First Order Methods For Reliability Based Optimization." *Journal of Mechanical Design*, Vol. 127, p. 851-857.
- Ditlevesen PG, and Bjerager P. (1988). "Plastic Reliability Analysis By Directional Simulation." *ASCE Journal of Engineering Mechanics*, Vol. 115, p. 1347-62.
- Eamon C, and Charumas B. (2011). "Reliability Estimation Of Complex Numerical Problems Using Modified Conditional Expectation Method." *Computers and Structures*, Vol. 89, p. 181-188.
- Eamon C, and Nowak, AS., (2005). "Effect of Edge-Stiffening and Diaphragms on the

- Reliability of Bridge Girders," Journal of Bridge Engineering, Vol. 10, No. 2, p. 206-214.
- Eamon C, Thompson M, and Liu Z. (2005). "Evaluation Of Accuracy And Efficiency Of Some Simulation And Sampling Methods In Structural Reliability Analysis." Structural Safety, Vol. 27, p. 356-392.
- Engelund S, and Rackwitz R. (1993). "A Benchmark Study On Importance Sampling Techniques In Structural Reliability." Structural Safety, Vol. 12. p. 255-276.
- George F. (2007). "Johnsons System of Distribution and Microarray Data Analysis." PhD Dissertation, Department of Mathematics, University of South Florida.
- Gomes HM, and Awruch AM. (2004). "Comparison Of Response Surface And Neural Network With Other Methods For Structural Reliability Analysis." Structural Safety, Vol. 26, p. 49-67.
- Haldar A, and Mahadevan S. (2000). "Probability, Reliability And Statistical Methods In Engineering Design." 1st ed. New York: John Wiley and Sons.
- Iman RL, and Conover WJ. (1982). "A Distribution-Free Approach To Inducing Rank Correlation Among Input Variables". Communications in Statistics, Vol. 11. p. 311-334.
- Karamchandani A, Bjerager P, and Cornell AC. (1989). "Adaptive Importance Sampling." Proceedings, International Conference on Structural Safety and Reliability (ICOSSAR), San Francisco, CA., p. 855-862.
- Karian ZA, and Dudewicz EJ. (2011). "Handbook Of Fitting Statistical Distributions With R." CRC Press.
- Karian ZA, and Dudewicz EJ. (2003). "Comparison of GLD fitting methods: Superiority of percentile fits to moments in L2 norm." Journal of the Iranian Statistical Society, Vol. 2, p. 171-187.

- Melchers RE. (1999) "Structural Reliability Analysis and Prediction." 2nd ed. New York: John Wiley & Sons.
- Ozaturk A, and Dale, RF. (1985). "Least Square Estimation Of The Parameters Of The Generalized Lambda Distribution." *Technometrics*, Vol. 27, p. 81-84.
- Rackwitz R, and Fiessler B. (1978). "Structural Reliability Under Combined Random Load Sequences." *Computers and Structures*, Vol. 9, p. 484-494.
- Rosowsky, D., Hassan, A., and Kumar, N. (1994). "Calibration of Current Factors in LRFD for Steel." *Journal of Structural Engineering*, Vol. 120, p. 2737-2746.
- Rubinstein RY. (1981). "Simulation And The Monte Carlo Method." 1st ed. New York: John Wiley & Sons.
- Slifker JF, and Shapiro SS. (1980). "The Johnson System: Selection And Parameter Estimation." *Technometrics*, Vol. 22, p. 239-246.
- Szerszen, MM. and Nowak, AS. (2003). "Calibration of design code for buildings (ACI 318): Part 2 - Reliability analysis and resistance factors." *ACI Structural Journal*, Vo.-1. 100, No. 3, p. 383-391.
- Wu YT. (1992). "An Adaptive Importance Sampling Method For Structural Systems Analysis, Reliability Technology." *ASME Winter Annual Meeting*, AD 28, p. 217-231.

List of Tables

Table 1. Random Variables for General Limit State Function

Table 2. Parameter Values for General Limit State Function

Table 3. Multiple Reliability Indices

Table 4. Maximum Function

Table 5. Displacement Limit State Function of Non-linear Static Truss

Table 6. Stress Limit State Function of Non-linear Static Truss

Table 7. Steel Frame Structure

Table 8. Complex Steel Frame Structure

List of Figures

Figure 1. Example PDFs of g and $R(x_i)$

Figure 2. Effect of Linearity on Accuracy

Figure 3. Effect of Linearity on Precision

Figure 4. Effect of Number of RVs on Accuracy

Figure 5. Effect of Number of RVs on Precision

Figure 6. Effect of Normality on Accuracy

Figure 7. Effect of Normality on Precision

Figure 8. Static Non-Linear Truss

Figure 9. Steel Frame Structure

Table 1. Random Variables for General Limit State Function

| Case | n | K | RVs |
|-----------------|-----|-----|---------------------------|
| 2 RV linear | 1 | 1 | d_i, w_j |
| 5 RV linear | 2 | 3 | d_i, w_{DLi}, w_{LLm}^* |
| 15 RV linear | 5 | 10 | d_i, w_{DLm}, w_{LLm}^* |
| 2 RV nonlinear | 1 | 1 | d_i, L_j |
| 5 RV nonlinear | 1 | 1 | d_i, w_j, L_j, E_j, I_j |
| 15 RV nonlinear | 3 | 3 | d_i, w_j, L_j, E_j, I_j |

Note: see eq. 7. $i=1$ to n and $j=1$ to k and indicate number of terms (RVs).

* $m=1-2$ for 5 RV linear case; $m=1-5$ for 15 RV nonlinear case.

Table 2. Parameter Values for General Limit State Function

| Parameter* | Value |
|------------|--|
| c | 5/384 |
| L_j | 6.1 (m) |
| E_j | 2×10^8 (kPa) |
| I_j | 6.452×10^{-4} (m ⁴) |
| w_j | 73600 (N/m) |
| w_{DL} | 19300 (N/m) |
| w_{LL} | 54300 (N/m) |

*within eq. 7, w may take the value of either w_j , w_{DL} , or w_{LL} , as shown in Table 1.

Table 3. Multiple Reliability Indices

| method | no. of calls | β | %err | Precision |
|----------------|--------------|---------|------|-----------|
| Exact solution | | 4.11 | -- | -- |
| FORM | -- | Fail | -- | -- |
| MCS | 1000 | N.F.* | -- | -- |
| NI | 1000 | 4.26 | 3.59 | 0.085 |
| GLD | 1000 | Fail | -- | -- |
| JSD | 1000 | 3.93 | 4.33 | 0.101 |
| GEV | 1000 | Fail | -- | -- |

* N.F. indicates no failures

Table 4. Maximum Function

| method | no. of calls | β | %err | Precision |
|----------------|--------------|---------|------|-----------|
| Exact solution | | 3.53 | -- | -- |
| FORM | -- | Fail | -- | -- |
| MCS | 1000 | N.F.* | -- | -- |
| NI | 1000 | 3.66 | 3.66 | 0.035 |
| GLD | 1000 | Fail | -- | -- |
| JSD | 1000 | 3.46 | 1.95 | 0.013 |
| GEV | 1000 | Fail | -- | -- |

* N.F. indicates no failures

Table 5. Displacement Limit State Function of Non-linear Static Truss

| method | nominal no. of calls | Actual no. of calls | % error tolerance | mean P=267 | | mean P=223 | | Correlated | |
|----------------|-------------------------|------------------------|----------------------|------------|------|------------|------|------------|------|
| | | | | β | %err | β | %err | β | %err |
| Exact Solution | | 1×10^9 | | 2.25 | -- | 3.59 | -- | 3.56 | -- |
| FORM | 150 | -- | -- | 1.96 | 12.9 | 3.12 | 13.1 | Fail | -- |
| MCS | 5000 | 5000 | | 2.54 | 11.4 | N.F. | -- | N.F. | -- |
| NI | 1000 | 5000 | | 2.04 | 9.33 | 3.50 | 2.50 | 2.66 | 25.3 |
| GLD | 1000 | 5000 | 3% | 2.34 | 3.85 | Fail | -- | Fail | |
| JSD | 1000 | 5000 | | 2.33 | 3.43 | 3.49 | 2.78 | 3.66 | 2.83 |
| GEV | 1000 | 5000 | | 2.38 | 5.46 | Fail | -- | Fail | -- |
| MCS | 8000 | 8000 | | 2.32 | 3.02 | N.F. | -- | | |
| NI | 1000 | 8000 | | 2.18 | 3.11 | 3.57 | 0.56 | | |
| GLD | 1000 | 8000 | 1% | 2.19 | 2.67 | Fail | -- | | |
| JSD | 1000 | 8000 | | 2.28 | 1.05 | 3.61 | 0.41 | | |
| GEV | 1000 | 8000 | | 2.34 | 3.85 | Fail | -- | | |

* N.F. indicates no failures

Table 6. Stress Limit State Function of Non-linear Static Truss

| method | nominal no. of calls | Actual no. of calls | % error tolerance | mean P=245 | | mean P=200 | | Correlated | |
|----------------|-------------------------|------------------------|----------------------|------------|------|------------|------|------------|------|
| | | | | β | %err | β | %err | β | %err |
| Exact Solution | | 1×10^9 | | 1.78 | -- | 3.79 | -- | 3.63 | -- |
| FORM | 250 | -- | -- | Fail | -- | Fail | -- | Fail | -- |
| MCS | 5000 | 5000 | | 1.87 | 4.81 | N.F. | -- | N.F. | -- |
| NI | 1000 | 5000 | | 1.92 | 7.30 | Fail | -- | 3.13 | 12.7 |
| GLD | 1000 | 5000 | 3% | 1.89 | 5.82 | Fail | -- | Fail | |
| JSD | 1000 | 5000 | | 1.85 | 3.78 | 3.91 | 3.07 | 3.51 | 3.31 |
| GEV | 1000 | 5000 | | 1.70 | 4.70 | Fail | -- | Fail | -- |
| MCS | 8000 | 8000 | | 1.77 | 0.56 | N.F. | -- | | |
| NI | 1000 | 8000 | | 1.86 | 4.30 | 3.17 | 16.3 | | |
| GLD | 1000 | 8000 | 1% | 1.79 | 0.83 | Fail | -- | | |
| JSD | 1000 | 8000 | | 1.75 | 1.46 | 3.82 | 0.78 | | |
| GEV | 1000 | 8000 | | 1.73 | 2.76 | Fail | -- | | |

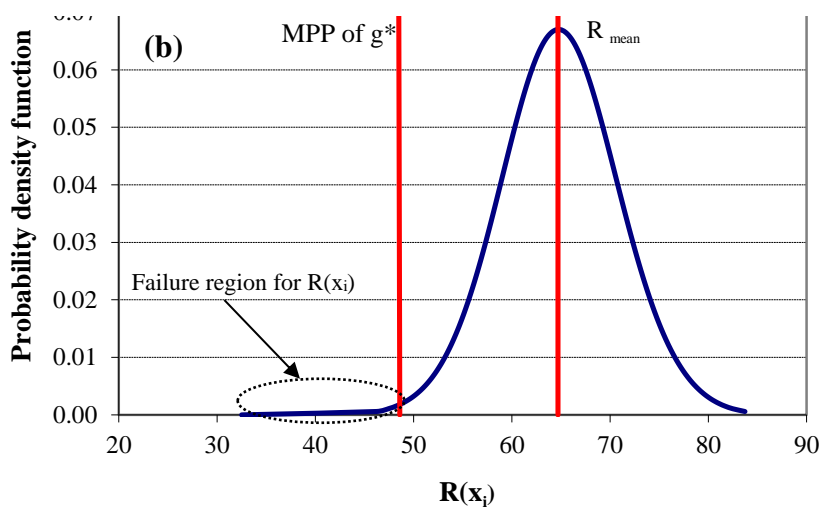
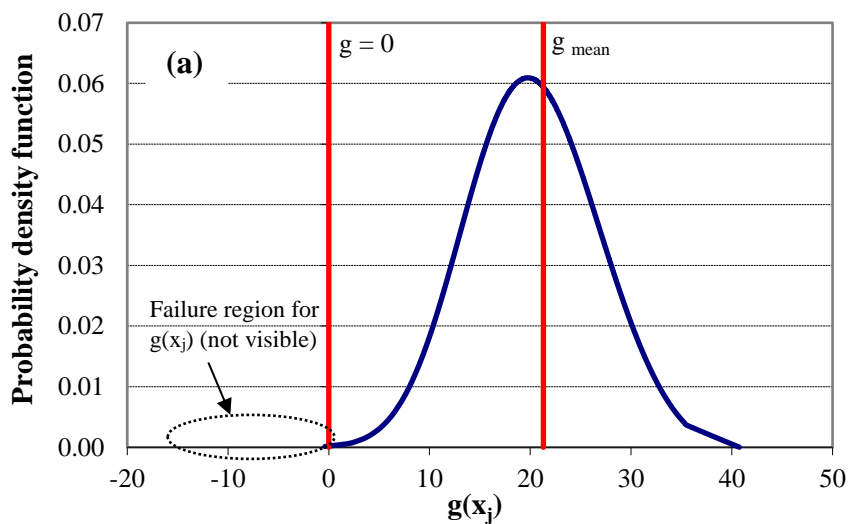
* N.F. indicates no failures

Table 7. Steel Frame Structure

| method | nominal | Actual | mean P = 400 | | mean P = 312 | |
|----------------|--------------|-----------------|--------------|------|--------------|------|
| | no. of calls | no. of calls | β | %err | β | %err |
| Exact Solution | | 1×10^9 | 1.803 | -- | 3.26 | -- |
| FORM | 150 | -- | 1.86 | 3.27 | Fail | -- |
| MCS | 7000 | 7000 | 1.82 | 0.93 | 3.10 | 5.16 |
| NI | 1000 | 7000 | 1.84 | 2.01 | Fail | -- |
| GLD | 1000 | 7000 | 1.89 | 4.85 | 3.52 | 7.38 |
| JSD | 1000 | 7000 | 1.76 | 2.55 | 3.14 | 3.68 |
| GEV | 1000 | 7000 | 1.82 | 0.44 | Fail | -- |

Table 8. Complex Steel Frame Structure

| method | nominal | Actual | 4 RVs | | 53 RVs | |
|----------------|--------------|-----------------|---------|------|---------|------|
| | no. of calls | no. of calls | β | %err | β | %err |
| Exact Solution | | 1×10^9 | 3.68 | -- | 3.70 | -- |
| FORM | 250 | -- | Fail | -- | Fail | -- |
| MCS | 7000 | 7000 | N.F. | -- | N.F. | -- |
| NI | 1000 | 7000 | Fail | -- | Fail | -- |
| GLD | 1000 | 7000 | Fail | -- | Fail | -- |
| JSD | 1000 | 7000 | 3.52 | 4.37 | 3.59 | 3.06 |
| GEV | 1000 | 7000 | Fail | -- | Fail | -- |



(a) Calculating p_f by sampling g directly results in a very small failure region. (b) Failure region by sampling $R(x_i)$.

Figure 1. Example PDFs of g and $R(x_i)$.

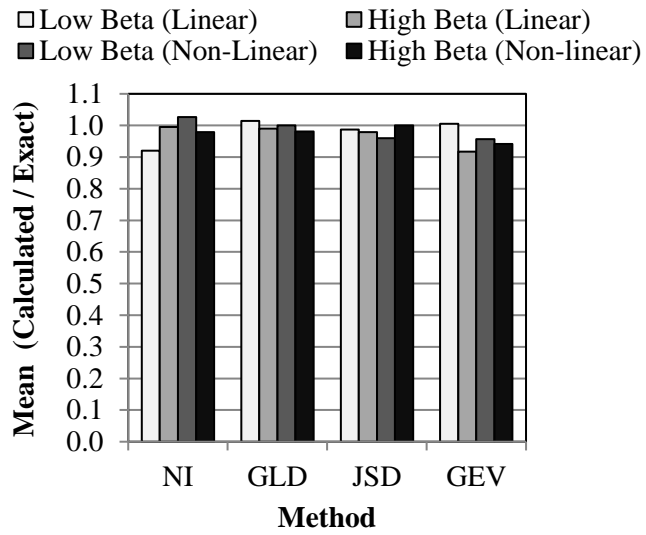


Figure 2. Effect of Linearity on Accuracy

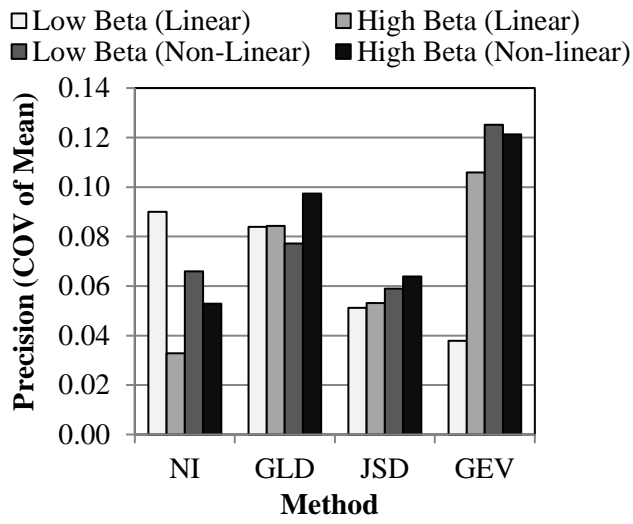


Figure 3. Effect of Linearity on Precision

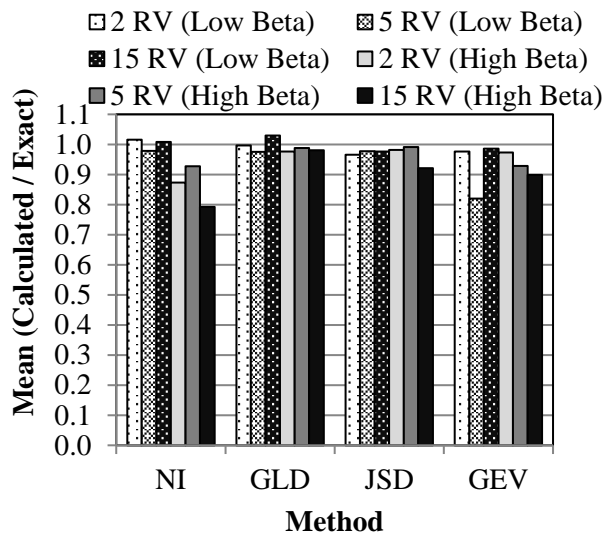


Figure 4. Effect of Number of RVs on Accuracy

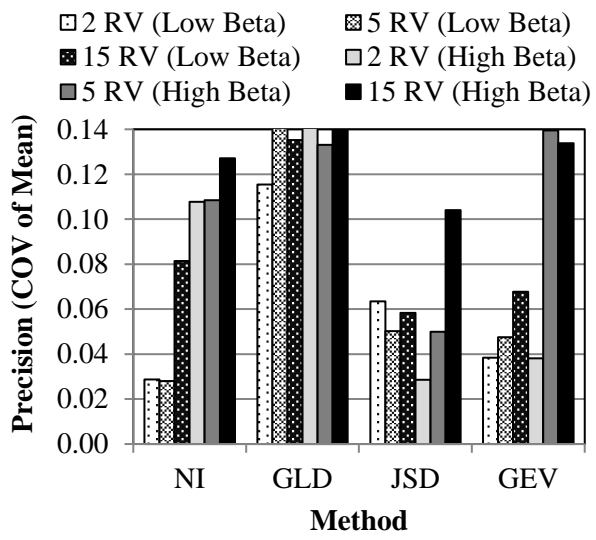


Figure 5. Effect of Number of RVs on Precision

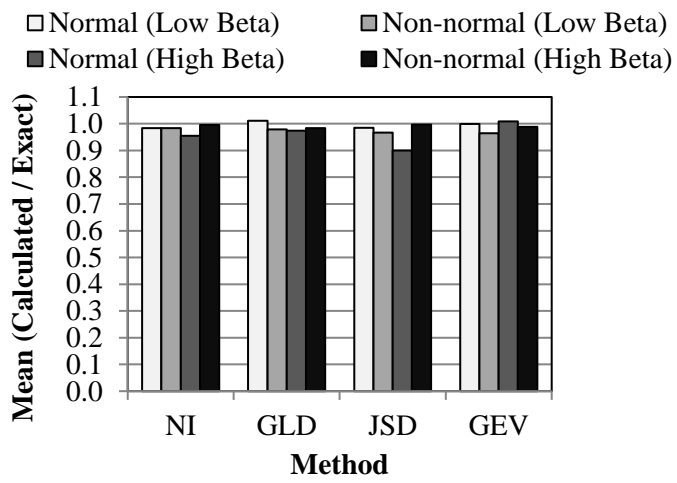


Figure 6. Effect of Normality on Accuracy

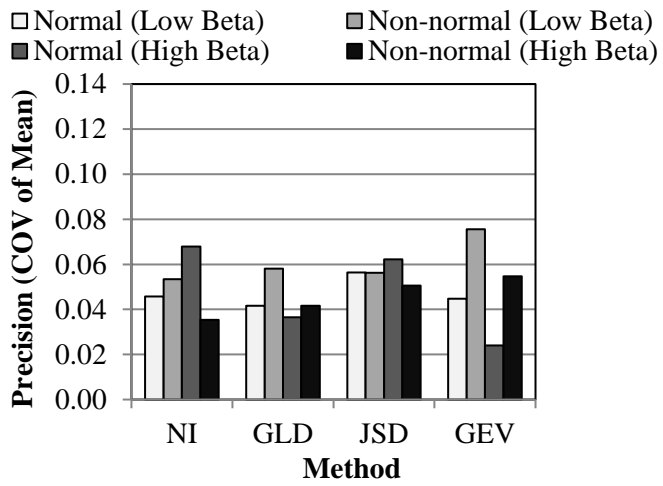


Figure 7. Effect of Normality on Precision

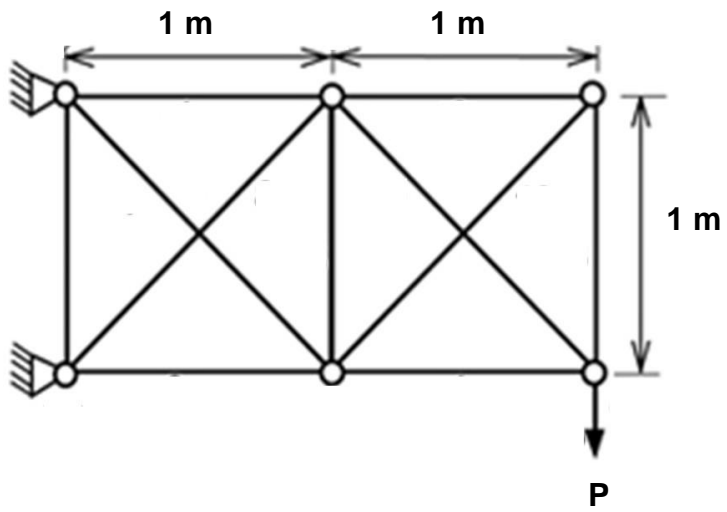


Figure 8. Static Non-Linear Truss

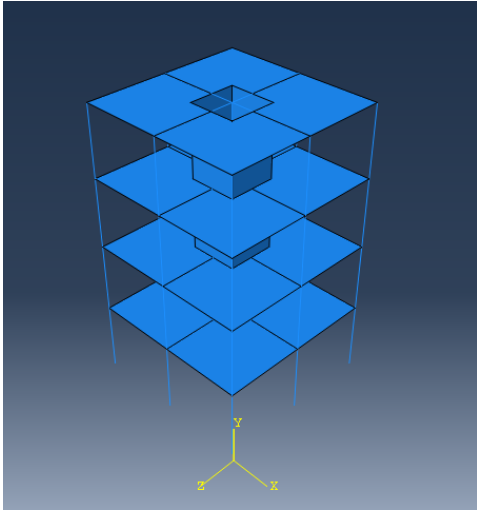


Figure 9. Steel Frame Structure